

Agnieszka BICZ¹, Wiesław BICZ¹, Marcin KORZENIOWSKI², Andrzej AMBROZIAK²

¹ PRZEDSIĘBIORSTWO BADAWCZO PRODUKCYJNE OPTEL Sp. z o.o.

30 Morelowskiego St., 52-429 Wrocław, Poland

² UNIVERSITY OF TECHNOLOGY IN WROCLAW, MECHANICAL ENGINEERING FACULTY,

DEPARTMENT OF MATERIALS SCIENCE AND WELDING STRENGTH, 5 Łukasiewiczza St., 50-371 Wrocław, Poland

An application of critically refracted longitudinal ultrasonic subsurface waves (L_{CR}) to industrial nondestructive testing of thin walled pipe shaped elements of shock absorbers, axle shafts and transmission shafts

Abstract

The paper describes the application of critically refracted longitudinal ultrasonic subsurface waves (L_{CR} , known also as lateral, creeping or head waves) to nondestructive flaw detection in friction welding or MAIB welded thin walled pipe shaped parts. The theory, a practical laboratory and industrial applications are presented.

Keywords: ultrasonic waves, subsurface waves, head waves, L_{CR} , creeping waves, flaw detection in friction butt welds, MIAB welding, ultrasonic testing of thin walled pipes.

1. Introduction

Contemporary ultrasonic testing methods allow detecting flaws that cannot be detected with other methods, such as dye penetrant inspection, magnetic particle testing, even not with X-ray tests. Their advantages are: very good detectability of flat flaws, cracks and lack of fusion (much better than in methods using radiation); the possibility to determine the position, type and size of flaw. Ultrasound allows also the detection of changes in material structure, grain size and physical properties of material. Actual trends in car industry are forcing the manufacturer of automobile components not only to improve their production process to be able to manufacture high quality parts with low costs, but also to make the weight of car lower. One of the possibilities are changes in manufacturing processes and the use of elements with thinner walls, but having the same strength. This is one of the reasons, why a movement toward having many advantages method of Magnetically Impelled Arc Butt (MIAB) welding is actually observed. Ultrasonic nondestructive testing is difficult if the wall thickness is lower than 3 mm, but especially in the case, if there is no easy access to the weld due to the too large scattering of the wave on molding protrusion. Due to this fact and small wall thickness, the use of ultrasonic subsurface waves seem to be the best suitable method of testing welds in shock absorbers, half axes and shafts.

2. Generation of subsurface waves

The wave is generated due to the transformation of a sound wave during the transmission through the contact surface of two media. If the immersion technique is used, it can be assumed that there is only a longitudinal wave in the fluid (I). Only the longitudinal wave is reflected. If the sound speed in fluid is lower than the speed of both sound waves in the solid (II), three critical angles are possible (θ' , θ'' , θ'''), and can be calculated with the help of the Snell's law:

$$\begin{cases} \theta' = \arcsin\left(\frac{c_0}{c_L}\right) \\ \theta'' = \arcsin\left(\frac{c_0}{c_T}\right), \\ \theta''' = \arcsin\left(\frac{c_0}{c_R}\right) \end{cases} \quad (1)$$

where:

c_0 – sound speed of the longitudinal wave in fluid,

c_T – sound speed of the shear wave in solid,

c_L – sound speed of the longitudinal wave in solid,

c_R – sound speed of Rayleigh (surface) waves.

Each critical angle corresponds to the case, where wave propagation is possible only along the border between the media. Under such conditions due to the superposition of volume and surface components, nonhomogeneous waves, known as leaky waves, are formed. The leaky subsurface waves are also called L_{cr} (critically refracted longitudinal), subsurface, head, creeping or lateral waves, since their propagation causes that the energy follows the surface curvature [1-4].

The attenuation and interference occurring in limited size beams cause that the pressure reflection coefficient significantly falls in the region of a critical angle [2, 3]. The mathematical model, proposed by Becker – Richardson [2], and Bertoni – Tamir [3] allows describing this effect with a large accuracy. It was not possible in the classical theory formulated by Schoch. This difference is shown in Fig. 1

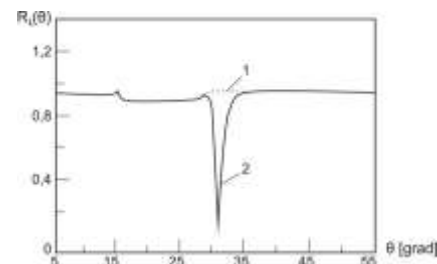


Fig. 1. Angular dependence of the pressure reflection coefficient according to the Schoch theory (dotted line 1) and experimental results for steel (solid line 2) [1]

Abrupt fall of the reflection coefficient in the region of the third critical angle corresponds to the generation of a subsurface wave – the energy is not reflected but propagates in the solid body.

Based on the parameters of the media (water (I) and steel (II), i.e.:

- Longitudinal wave for II: $V_l = 5900 \frac{m}{s}$
 - Shear wave for II: $V_s = V_l \sqrt{\frac{1-2\sigma}{2(1-\sigma)}} = 3260 \frac{m}{s}$ – value calculated for the Poisson coefficient $\sigma = 0.28$
 - Rayleigh wave for II: $V_R \approx 0.93V_s = 3032 \frac{m}{s}$
- it is possible to calculate the third critical angle: 31.5° .

3. Generation of subsurface waves (L_{RC}) in simulations based on the finite elements method (FEM) in comparison with experimental results

For simulations based on FEM freely available software SimSonic [5] was used. It allows the calculation of sound wave propagation based on finite-difference time-domain (FDTD) computations of the elastodynamic equations (speed and stress).

Let a thin walled steel pipe of a shock absorber be our test object. It contains an especially made crack. The sound wave, generated by a focused ultrasonic transducer with the medium

frequency of 10 MHz is falling on the surface of the pipe under the angle of 31 degrees (Fig. 2, 3). We will simulate the generation of the subsurface wave with FEM.

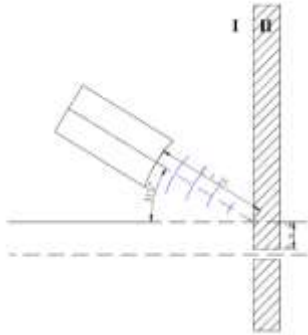


Fig. 2. Schematic of the measuring system, ultrasonic transducer under 31° (water (I) – steel (II))

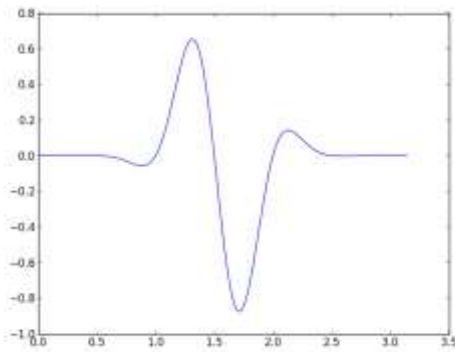


Fig. 3. The source of stress – pulse generated by the ultrasonic transducer 10 MHz

An ultrasonic wave is a mechanical wave. In the nondestructive testing, its amplitude is small. This allows using the Hooke’s law:

$$\frac{F}{S} = E \frac{\Delta l}{l}, \tag{1}$$

where:

- F – force, N
- S – surface, m^2
- E – Young module, Pa
- Δl – extension of the volume element, m
- l – initial element length, before the force was applied, m.

Based on the above, the strain is defined as a quotient of the force and surface:

$$\sigma = \frac{F}{S}, \tag{2}$$

For stress measurement, the surface $S \neq 0$ is assumed. In the FEM calculation S must be small enough to be able to treat the object as continuous.

3.1. 2D Simulation based on the finite elements method (FEM)

In two dimensional calculations (2D), the simplest case is a mesh based on squares. The metric of such a mesh is Δx .

If the sound wave should be simulated Δx must be two powers smaller than the wave length. Fig. 4. shows the coordinate system with stress and speed components with the space step Δx , that is dividing volume to mesh (Fig. 5). The calculations were made for the boundary condition PML [5 page 14], for the frequency of 10 MHz, $\Delta x = 0.05$ mm, the maximum speed of 7000 m/s (for calculations the higher speed than that in reality was assumed), the

time step was calculated by the software as [5 page 13] for $\alpha = 0.99$:

$$\Delta t = \alpha \frac{\Delta x}{\sqrt{2}V_{max}}, \tag{3}$$

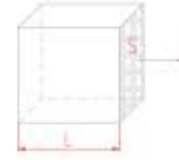


Fig. 4. Extended element with square shape

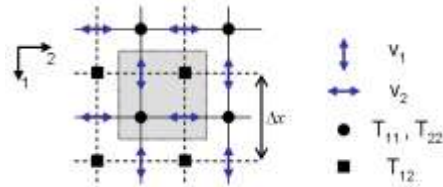


Fig. 5. Speed and stress in the mesh [5]

Elasticity modules C_{ji} [6] for water (I) and steel (II) are given in Table 1:

Tab. 1. Elasticity modules for (I) and (II)

Parameters	Water (I)	Steel (II)
Density (ρ)	$1 \frac{kg}{m^3}$	$7280 \frac{kg}{m^3}$
Young module	1	210 GPa
Poisson coefficient	1	0.28
Velocity of longitudinal wave V_l	$1485 \frac{m}{s}$	$5900 \frac{m}{s}$
C_{11}	2.25	268.5 GPa
C_{22}	2.25	268.5 GPa
C_{12}	2.25	104.4 GPa
C_{66}	2.25	82.0 GPa

A symmetrical stress tensor of the physical model is expressed by [5]:

$$\begin{bmatrix} \frac{\partial T_{11}}{\partial t} \\ \frac{\partial T_{22}}{\partial t} \\ \frac{\partial T_{12}}{\partial t} \end{bmatrix} = \begin{bmatrix} c_{11} & c_{12} & 0 \\ c_{12} & c_{22} & 0 \\ 0 & 0 & c_{66} \end{bmatrix} \begin{bmatrix} \frac{\partial v_1}{\partial x_1} \\ \frac{\partial v_2}{\partial x_2} \\ \frac{\partial v_2}{\partial x_1} + \frac{\partial v_1}{\partial x_2} \end{bmatrix}, \tag{5}$$

where:

- T_{11}, T_{22}, T_{12} – stresses in different direction of the mesh
- V_1, V_2 – local sound speed in different directions:

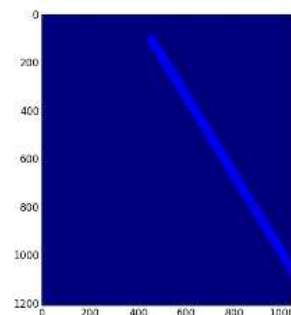


Fig. 6. Model of the measured object, the steel pipe placed under 31.5° angle in the distance of 21 mm from the stress source (see Fig. 2)

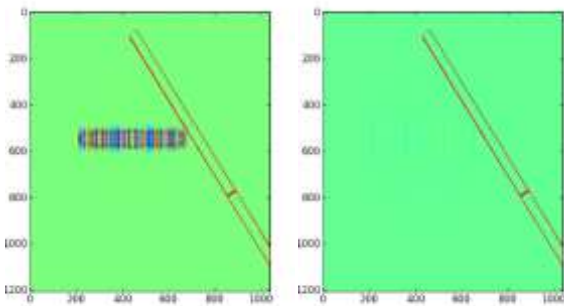


Fig. 7. Stress T11 (generation of creeping wave L_{CR}) (left side simulation after 8 μs; right side after 9 μs)

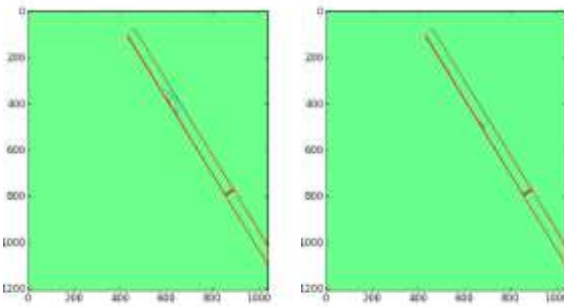


Fig. 8. Stress T12 (generation of creeping wave L_{CR}) (left side simulation after 8 μs; right side after 9 μs)

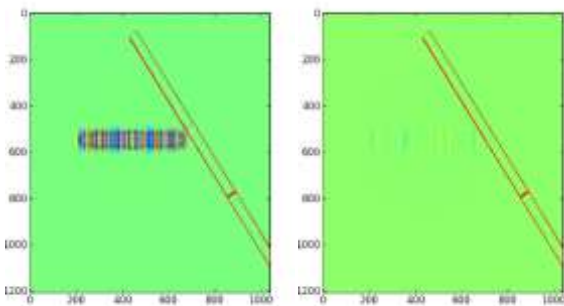


Fig. 9. Stress T22 (generation of creeping wave L_{CR}) (left side simulation after 8 μs; right side after 9 μs)

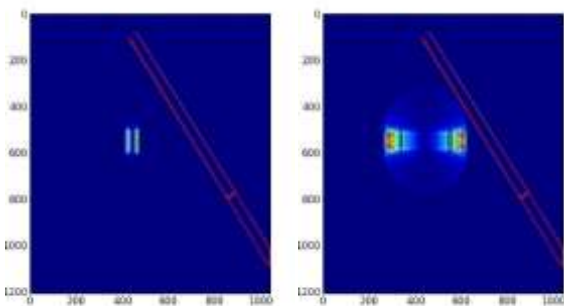


Fig. 10. Visualization of local speed *V*, (left after 0 μs; right after 6 μs)

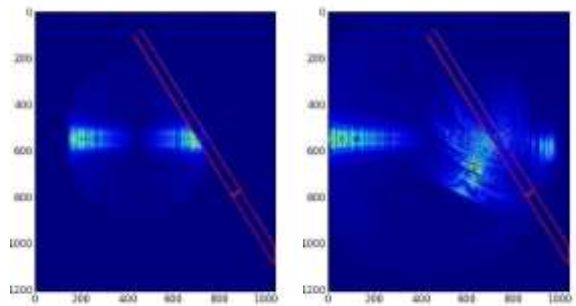


Fig. 11. Visualization of local speed *V*, (left after 8 μs; right after 9 μs)

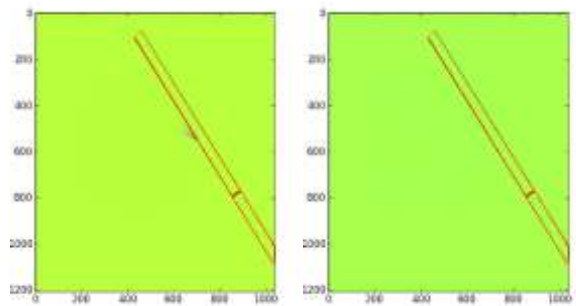


Fig. 12. Visualization of local speed *V*, (left after 9 μs; right after 10 μs)

3.2. 3D Simulation based on the finite elements method (FEM)

In three dimensional calculations (3D), the simplest case is a mesh based on squares (Fig 13). The metric of such a mesh is Δ*x*:

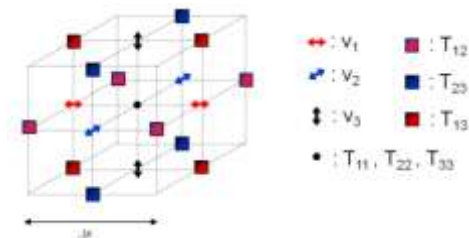


Fig. 13. Speed and stress in the mesh [5]

The calculations were made for the boundary condition PML [5 page 14], a frequency of 1 MHz, Δ*x* = 0.1 mm, the maximum speed of 7000 m/s, the time step was calculated by the software as [5 page 13] for α = 0.99:

$$\Delta t = \alpha \frac{\Delta x}{\sqrt{3}V_{max}}, \quad (6)$$

Elasticity modules *C_{ji}* [6] for water (I) and steel (II) are given in Table 1.

To minimize the size of the mesh, only a part of the pipe in the surroundings of the flaw was taken into account in the calculation. It caused that the calculation was quicker. This part of the pipe (this could be a part of e.g. half axe), placed under the angle is schematically shown in Fig 14.

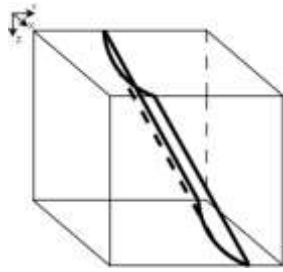


Fig. 14. Schematic picture of the pipe

The cross section XY on a chosen height z equal to 0, 125 and 131 is shown in Fig. 14. The steel is shown as a white line. It moves from picture to picture due to the inclination angle, Fig 15. One can also see a flaw, perpendicular to the surface of steel. Since it is also under some angle in relation to the cutting surface, it is visible on two figures below.



Fig. 15. Cross section XY on chosen height z equal 0, 125 and 131

Due to the limitations of the 3D mesh, the simulation was made at 1 MHz frequency (Fig. 3).

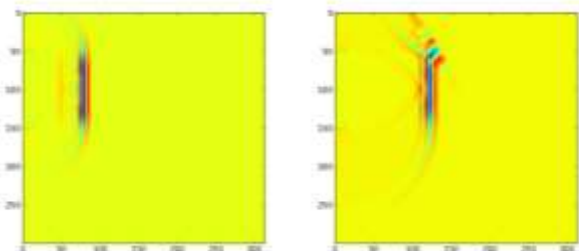


Fig. 16. Visualization 2D of the surface $Z=125$. 1 MHz is generated in water, simulation time $6 \mu s$ and $9 \mu s$

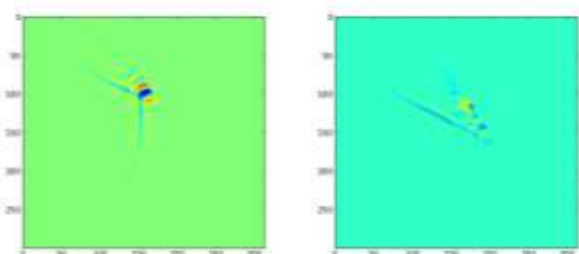


Fig. 17. Visualization 2D of the surface $Z=125$. 1 MHz wave is generated in water, simulation time $11 \mu s$ and $13 \mu s$. The subsurface and reflected waves are visible

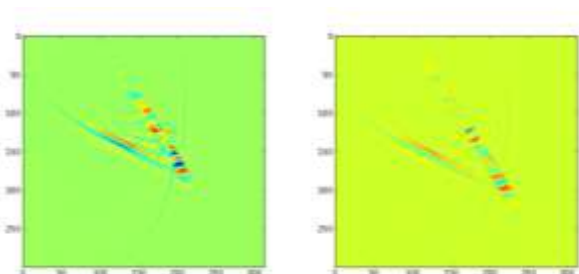


Fig. 18. Visualization 2D of the surface $Z=125$. 1 MHz wave is generated in water, simulation time $14 \mu s$ and $15 \mu s$. The subsurface wave reflected from the flaw and the wave reflected from the steel surface are visible

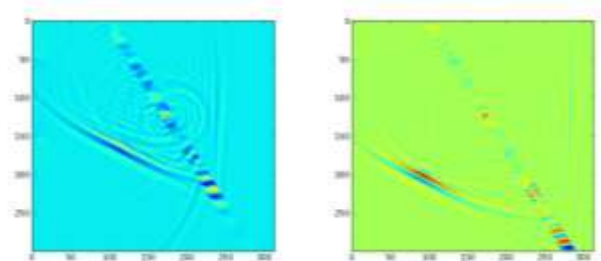


Fig. 19. Visualization 2D of the surface $Z=125$. 1 MHz wave is generated in water, simulation time $16 \mu s$ and $19 \mu s$. The subsurface wave reflected from the flaw is visible

Fig. 20 shows the subsurface wave generated in the 3D visualization. The steel is shown as a dark surface, the bright spot is the flaw.



Fig. 20. 3D visualization. Generation of the subsurface wave, simulation time $11 \mu s$

Fig. 21 shows the cross section of both the wave and the steel mesh. The wave reflected from the surface is visible:



Fig. 21. 3D visualization. Generation of the subsurface wave, simulation time $11 \mu s$



Fig. 22. Reflection of the subsurface wave from the flaw. Simulation time $15 \mu s$. The subsurface, transmitted and reflected from the steel surface waves are visible

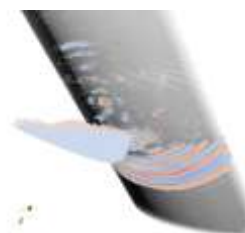


Fig. 23. Reflection of the subsurface wave from the flaw. Simulation time $16 \mu s$. The subsurface, transmitted and reflected from steel surface waves are visible

3.3. Conclusions from the 2D and 3D simulations based on the finite elements method (FEM)

Generation of an ultrasonic wave is possible, because some stress is caused by the electrical excitation of an ultrasonic transducer. In the pulse-echo mode, it sends and receives the wave on the same surface. In simulations, there is no object corresponding to the transducer. The stress is generated numerically directly in the medium in the part of the mesh, having parameters corresponding to water. To be able to simulate the work of the transducer, the 3D data are collected with 0.1 μs step and only the data corresponding to the surface are cut out from the 3D matrix. This causes, that a 2D matrix is generated for each time step. After it, the results were averaged for each 2D matrix and shown depending on time. The result is the 3D matrix, where two indexes are connected with the dimensions and one with time. In a real transducer, there is additionally the conversion from the stress to the voltage.

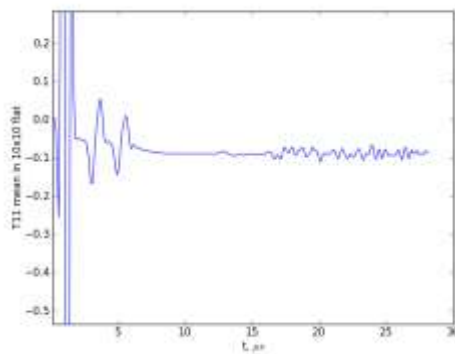


Fig. 24. Reflection of the subsurface wave from the flaw

4. Experimental verification of the simulation results

The simulated conditions were repeated in a real measuring system, according to Fig. 2. The ultrasonic transducer with 10 MHz medium frequency and 21 mm focus distance was used. The diameter of the focal spot was around 0.4 mm, its length around 6 mm. An ultrasonic card OPCARD from the company PBP Optel sp. z o. o. was used as a sender and data acquisition system. During measurements the transducer was placed in relation to the pipe surface under the angle of $\alpha_{CR}=31.5^\circ$. The ultrasonic beam was focused on the surface of the pipe around $h \approx 4$ mm from the weld.

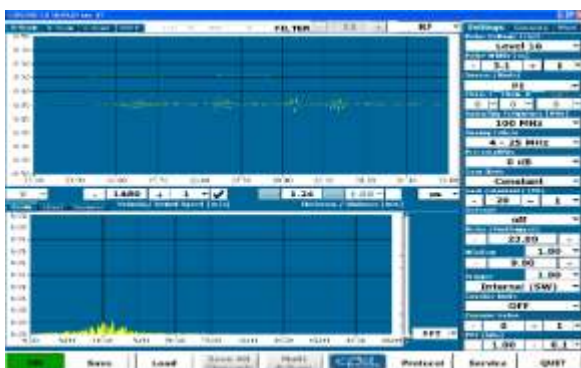


Fig. 25. A-scan. No flaw detected. The ultrasonic wave reflected from the protrusion

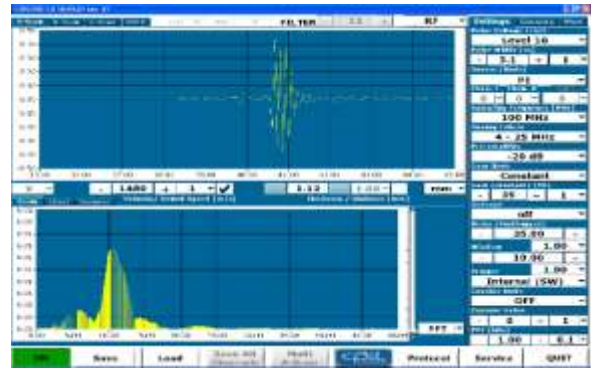


Fig. 26. A-scan. The ultrasonic wave reflected from the flaw



Fig. 27. B-scan. The ultrasonic wave reflected from the flaw

To be able to check the depth of the intrusion of the subsurface wave, the tests with plate having holes with different depths were made. The steel plate with dimensions 60 mm × 30 mm × 8 mm with the following sound speeds was used:

- Longitudinal wave $V_L = 5900 \frac{m}{s}$ – measured
- Shear wave $V_S = V_L \sqrt{\frac{1-2\sigma}{2(1-\sigma)}} = 3260 \frac{m}{s}$ – calculated from the Poisson coefficient $\sigma = 0.28$
- Rayleigh wave $V_R \approx 0.93V_S = 3032 \frac{m}{s}$ – calculated

The holes in the plate had the depths from 1 mm to 7.9 mm. Experiments were made with the focused transducer described above (10 MHz medium frequency, 21 mm focus distance, diameter of the focal spot 0.4 mm, its length around 6 mm). The inclination angle in relation to the plate surface $\alpha_{CR}=31.5^\circ$. The ultrasonic beam was focused under the polished surface of the metal without holes as shown in Fig. 28.

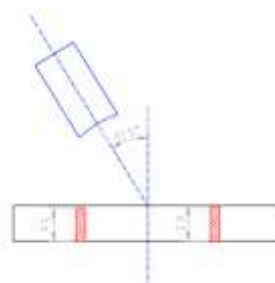


Fig. 28. Steel plate with holes and position of the ultrasonic transducer

On the boundary between water and steel – as stated before – both subsurface and Rayleigh waves are generated. The Rayleigh waves are very well suitable for the detection of surface defects, but in the depth corresponding to one wave length $\lambda_R = 0.3$ mm their amplitude falls to around 19%. This is the reason why they are not suitable for investigations of objects lying in larger depths. The subsurface waves, propagating parallel to the plate surface are

leaking volume waves into both mediums. In water, it is a longitudinal wave, in steel both: a pressure and shear wave. In comparison to the Rayleigh wave the attenuation of the subsurface wave does not depend on the surface roughness. Its amplitude falls with a distance according to the following formula [6]:

$$A = \frac{l}{x^2}, \quad (4)$$

The inclination angle used in the experiment $\alpha_{CR}=31.5^\circ$ corresponds to the angle with the maximum transmission of sound energy to the subsurface wave through the boundary water – low carbon steel [1]. The wave is reflected by the holes and propagates parallel to the surface, leaking its energy in each point on its way [7, 8].

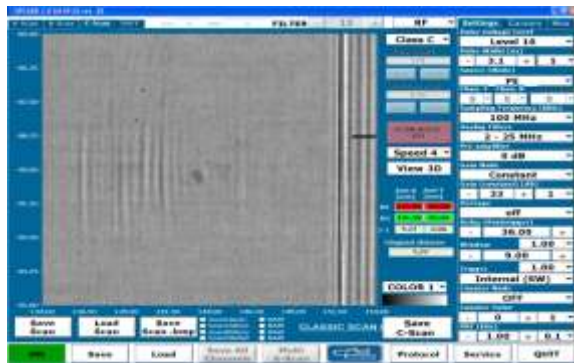


Fig. 29. 2D C- scan of the surface of the measured plate

Between the markers in Fig. 29, more signals are visible. On the right side of the picture, the reflection from the plate boundary is visible.

In Fig. 30, two strongest signals are marked. In the following pictures, A-scans of the signals in the marked points are shown.



Fig. 30. 2D C- scan of the measured plate



Fig. 31. A- scan. The signal obtained at the point marked with the red marker in Fig. 30



Fig. 32. A- scan. The signal obtained at the point marked with the green marker in Fig. 30



Fig. 33. B- scan for the line with the hole

5. Application of the subsurface waves in an industrial system for nondestructive testing of elements of shock absorbers

The measuring system opStrut is designed for automatic nondestructive ultrasonic immersion testing of quality of butt welds in strut rods used in shock absorbers – directly after the manufacturing process. Each produced element is controlled. The device uses the above described subsurface waves, propagating in the pipe wall of the measured element.

The device is able to check automatically the type of an element and adjusts the measurement procedure according to its shape. Each detail is dried after removing from the machine. The occurrence of a flawed element is signaled by a red light and information on the operator panel. Such a detail is also marked mechanically and the work of the machine is stopped until such an element is not stored in a special container. The measurement results are stored in the device memory, generating error statistic that can be used for improvement of the production process. The statistics contains also information about the measurement time and the operator which has made the measurement. The device contains the software equipped with flaw evaluation criteria, based on the experience with similar equipment and the previously made measurements. This criteria can be changed by the user, based on the experience collected during the work with the device. The device does not require the removal of the weld protrusion.

The system for controlling friction welds in strut rods of shock absorbers (Fig. 34) contains the following modules:

- detection of a strut rod inserted in the device;
- type detection, adjustment of the measurement procedure and check if the element is correctly inserted;
- detection of manipulation during the measurement,
- water resupplying module which also checks its cleanliness.

Water circulates between two containers that can be filled up or emptied without the need of removing them – they are equipped with inlets and outlets, secured during the normal work of the

machine. The inlet is equipped with a filter which prevents the introduction of solid particles that could disturb the work of the measuring system.



Fig. 34. Device for nondestructive ultrasonic testing of friction welds "opStrut" made by PBP Optel Sp. z o.o. for company BWI in Krosno (Poland)

6. Conclusions

It has been shown that the construction of an ultrasonic nondestructive measuring system which allows the detection of flaws in thin walled pipes using the subsurface waves generated with beams propagating at the critical angle in relation to the surface is possible. The system was successfully used in the industrial application. This technique allows e.g. the detection of flaws in friction welds made in such pipes. The theory explaining the method used is presented and calculations based on FEM described. The industrial machine using this technique has been presented.

The method can be used in the cases where flaws close to the surface and in elements with thin walls should be detected, especially for flaw detection in friction or MAIB welded thin walled pipe shaped parts.

This research project was co-funded by NCBiR (Polish National Centre for Research and Development in the third competition of the Applied Research Program (PBS) - Criteria and methodology of quality control of joints made with magnetically impelled arc.

7. References

- [1] Awram Lewi: Ultradźwiękowe badania nieniszczące własności mechanicznych cienkich elementów konstrukcyjnych. Instytut Podstawowych Problemów Techniki Polskiej Akademii Nauk, Warszawa 2010, s. 93-103.
- [2] Becker F., Richardson R.: In Research Technique in NDT, Ed. R.Sharpe; Academic Press Publ., New York, s. 91-130.
- [3] Bertoni H., Tamir T.: Unified Theory of Rayleigh-Angle Phenomena for Acoustic Beam at Liquid-Solid Interfaces; J. Appl. Physics, 1973, p. 157-172.
- [4] Tiersten H.: Elastic Surface Waves Guided by Thin Films. J. Appl. Physics, 1969, p. 770-791.
- [5] Manual for SimSonic, http://www.simsonic.fr/downloads/SimSonic2D_UserGuide.pdf, access at day 2016-07-15
- [6] Deputat J.: Fale podpowierzchniowe. Seminarium Badań Nieniszczących, Zakopane, marzec 2006, s. 1, 6 – 7.

- [7] Neubauer W. G., Uginčius P., Überall H.: Theory of Creeping Waves in Acoustic and Their Experimental Demonstration. Zeitschrift für Naturforschung A, Volume 24, Issue 5, p. 697 – 700.
- [8] Ying C. F., Zhang S. Y., Wang L. S.: Study on the Creeping Waves Around Cylindrical Cavities in Solid Medium by the Photoelastic Technique. Scientia Sinica XXIV, 1981, pp. 1512 - 1516.
- [9] Śliwiński A.: Ultradźwięki i ich zastosowanie. WNT 2001, s.26-31.

Received: 15.04.2016

Paper reviewed

Accepted: 01.06.2016

Agnieszka BICZ, MSc

Graduate of Technical University in Wrocław, department Electronics and Telecommunication, since 1993 she works at R&D laboratory of OPTEL Sp. z o.o. where she is developing advanced industrial and laboratory systems for quality control and support of technological processes, based on ultrasonic technology. Has made significant experience with weld control systems and biometrics.



e-mail: A.Bicz@optel.pl

Wiesław BICZ, MSc

Graduate of Technical University in Wrocław with a specialty coherent optics. Inventor and founder of PBP Optel. Since 1985 he is working in the area of ultrasonic technology, with special application in finger recognition.



e-mail: W.Bicz@optel.pl

Prof. Andrzej AMBROZIAK, DSc, eng.

Vice-Dean of the Faculty of Mechanical Engineering Technical University of Wrocław, Vice Head of the Department of Strength of Materials and Welding. Research work includes the study of processes of welding in particular friction welding arc, welding and other joining processes.



e-mail: andrzej.ambroziak@pwr.edu.pl

Marcin KORZENIOWSKI, PhD, eng.

Assistant Professor in the Department of Materials Science and Welding Strength of Wrocław University of Technology. Scientific activities and research work covers the basic techniques in the field of welding, in particular welding and robotic welding, welding process automation and quality control of welded joints non-destructive methods - mainly ultrasonic testing.



e-mail: marcin.korzeniowski@pwr.edu.pl